

Directional solidification and characterization of NiAl–9Mo eutectic alloy

Jian-fei ZHANG^{1,2}, Jun SHEN¹, Zhao SHANG¹, Lei WANG¹, Heng-zhi FU¹

1. State Key Laboratory of Solidification Processing, Northwestern Polytechnical University, Xi'an 710072, China;
2. College of Material and Metallurgy, Inner Mongolia University of Science and Technology, Baotou 014010, China

Received 20 January 2013; accepted 13 April 2013

Abstract: Ni–45.5Al–9Mo (mole fraction, %) alloy was directionally solidified with a constant temperature gradient ($G_L=334$ K/cm) and growth rates ranging from 2 to 300 $\mu\text{m/s}$ using a Bridgman type crystal growing facility with liquid metal cooling (LMC) technique. The effect of growth rate (v) on the solidified microstructures such as rod spacing (λ), rod size (d) and rod volume fraction was experimentally investigated. Two types of the solidified interfaces, planar and cellular, were identified. On the condition of both planar and cellular eutectic microstructures, the relationships between λ , d and v were given as: $\lambda v^{1/2}=5.90 \mu\text{m}\cdot\mu\text{m}^{1/2}\cdot\text{s}^{1/2}$ and $d v^{1/2}=2.18 \mu\text{m}\cdot\mu\text{m}^{1/2}\cdot\text{s}^{1/2}$, respectively. It was observed that the volume fraction of Mo phase could be adjusted in a certain range. The variation of phase volume fraction was attributed to undercooling increase and the growth characteristics of the individual constituent phases during the eutectic growth.

Key words: NiAl–9Mo; directional solidification; intermetallics; crystal growth; microstructure

1 Introduction

Alloys based on the intermetallic compound NiAl have recently attracted much attention because of their high melting point, low density, good environmental resistance, high thermal conductivity and attractive modulus [1–3]. However, their low ductility and fracture toughness at ambient temperature and inadequate strength and creep resistance at elevated temperature restrict their utilization. Accordingly, considerable efforts have been devoted to improving the mechanical behavior of NiAl alloys through grain refinement, micro- and macro-alloying, incorporating second phase reinforcements, mechanical alloying to produce dispersion strengthened NiAl [4–7].

A promising method of obtaining NiAl-based alloys with improved mechanical properties is the use of directional solidification (DS) of eutectic alloys, which would generate a composite structure formed by NiAl and another phase. According to previous works, many refractory transition metals, such as Cr, Mo, W, V, can form in situ eutectic composites with NiAl [8–11]. This may result in regular structures of fibrous or lamellar

type, and can significantly improve the mechanical properties of NiAl. More recent works on the NiAl–Mo system have shown that a fine dispersion of oriented ductile Mo fibers in NiAl can be achieved in NiAl–9Mo eutectic alloys by DS techniques. ZHANG et al [12] observed that the DS NiAl–Mo eutectic alloy can improve the room temperature fracture toughness, and the same has been demonstrated in the same system by MISRA et al [13]. BEI and GEORGE [14] studied the NiAl–Mo system, which displayed a rod-type eutectic microstructure, exhibited an increase in high-temperature strength with decreasing of the microstructural scale. FERRANDINI et al [15] also investigated the influence of growth rate on the mechanical behavior of NiAl–Mo eutectic alloy, and found that the well aligned eutectic microstructure led to higher strength level at room temperature.

It is well known that the mechanical properties of eutectic in situ composites sensitively depend on the eutectic spacing and morphology which can be controlled by processing parameters, such as temperature gradient and growth rate. Till now, little work has been reported about the microstructure characteristics of directionally solidified NiAl–9Mo alloy in a wide range

Foundation item: Project (51074128) supported by the National Natural Science Foundation of China; Project (2007ZF53067) supported by the Aeronautical Science Foundation of China; Project (2010JM6002) supported by the Natural Science Foundation of Shaanxi Province of China; Project (2012NCL004) supported by the Innovation Foundation of Inner Mongolia University of Science and Technology

Corresponding author: Jun SHEN; Tel: +86-29-88494708; E-mail: shenjun@nwpu.edu.cn

DOI: 10.1016/S1003-6326(13)62894-0

of growth rate. Based on the works of above mentioned, in the present work, the solidification behavior and microstructural characteristics of NiAl–9Mo eutectic alloy are investigated. So the influence of the growth conditions on material performance can be established. The solid/liquid (S/L) interface morphology, the eutectic spacing (λ), the fiber size (d) and the volume fraction of Mo fibers on the growth rate (v) at a constant temperature gradient are discussed in detail. In addition, as a regular eutectic alloy system, the experimental results are compared with the previous experimental results and the existing theoretical model.

2 Experimental

The master alloy with composition of Ni–45.5Al–9Mo (mole fraction, %) was prepared by induction melting under Ar atmosphere and dropped into a cylindrical ingot measuring 80 mm in diameter and 100 mm in length. The purity of raw materials used in this work is Ni 99.99% (mass fraction), Al 99.99% and Mo 99.95%, respectively. DS rods were cut from the master ingot into cylinder bars of $d3.9 \text{ mm} \times 100 \text{ mm}$ by wire electro-discharged machine (EDM) and placed into a high purity alumina crucibles of 4 mm inside diameter and 5 mm outside diameter. DS experiments were performed under an argon atmosphere in a Bridgman type crystal growing facility with liquid metal cooling (LMC) technique. The alumina crucible with the as-cast rod was positioned in the furnace and heated up to $(1973 \pm 10) \text{ K}$ with graphite heater by induction heating and then kept for 20 min for melt homogenization. The upper part with the heating element was then slowly and uniformly shifted downwards to allow unidirectional heat extraction. This operation was controlled by a servomotor at various withdraw rates. After the solidified distance reached 50 mm, the sample was quenched into liquid Ga–In–Sn alloy to obtain the interface growth morphology and study the formation of microstructure. A thermal gradient at the S/L interface was approximately 334 K/cm. The eutectic alloy samples were grown at different rates varying from 2 to 300 $\mu\text{m/s}$. Here, it's assumed that the growth rate was equal to the externally imposed velocity.

After melting, the directionally solidified samples were sectioned transversely and longitudinally by EDM for metallographic analysis. Metallographic process involved grinding, mechanical polishing and chemical etching with a solution of 80% $\text{HCl} + 20\% \text{HNO}_3$. The etched specimens were revealed and analyzed by a Lecia DM4000M optical microscopy (OM) and scanning electron microscopy (SEM) equipped with energy dispersive spectrometry (EDS). The quantitative image analysis was conducted by means of SISCAS V8.0

metallographic image analysis software. The eutectic spacing (λ) of the alloys was measured using the line-intercept method. The SEM images were quantitatively analyzed to determine the volume fraction of Mo fibers, fiber spacing and fiber size. About 300 individual rod spacings and 100 individual rod sizes (average edge length of the square cross-sections) for each examined velocity were measured to determine the spacing distribution and the rod scale.

3 Results and discussion

3.1 Steady-state S/L interface morphologies

Figure 1 shows a sequence of the S/L interface morphologies under steady-state at different growth rates. The eutectic microstructure was formed by the NiAl (matrix phase) and Mo phases (fiber phase). It can be seen from Figs. 1(a)–(c) that the S/L interfaces were planar under the growth rates in the range from 2 to 35 $\mu\text{m/s}$. As shown in Fig. 1(d), at $v=40 \mu\text{m/s}$, the Mo phase and NiAl phase were unstable, and two-phase eutectic cells appeared at the interface. When the growth rate increased to 100 $\mu\text{m/s}$, the fluctuation of interface became deteriorative and formed fully cellular interface as shown in Fig. 1(e). With the further increase in growth rate ($v=300 \mu\text{m/s}$), the S/L interface became a thick cellular one, and eutectic microstructures became irregular, as shown in Fig. 1(f). So it can be concluded that on the condition of $G_L=334 \text{ K/cm}$, the critical growth rate of directionally solidified NiAl–9Mo eutectic alloy remaining planar interface is 35–40 $\mu\text{m/s}$ which is higher than that in the studies of BEI and GEORGE [14] and FERRANDINI et al [15]. Apparently, this fact comes from the S/L interface stability under a higher temperature gradient. It is also clearly observed that with the variation of growth rate, the microstructure regularity and uniformity showed strong dependence on the growth rate. It is well established that the S/L interface has a significant impact on the final fibrous structure since the fiber/matrix interface is usually normal to the S/L interface during eutectic growth in order to minimize energy [16].

Maintaining planar interface is especially important when it is required to control the orientation of the phases in order to obtain in situ composites. Based on the theory of constitutional undercooling, the approximate criterion for stability of the eutectic S/L interfaces in this case can be expressed as follows [17]:

$$\frac{G_L}{v} \geq -\frac{m_L (C_E - C_0)}{D_L} \quad (1)$$

where G_L is the temperature gradient in the liquid ahead of the interface; v is the growth rate; m_L is the slope of

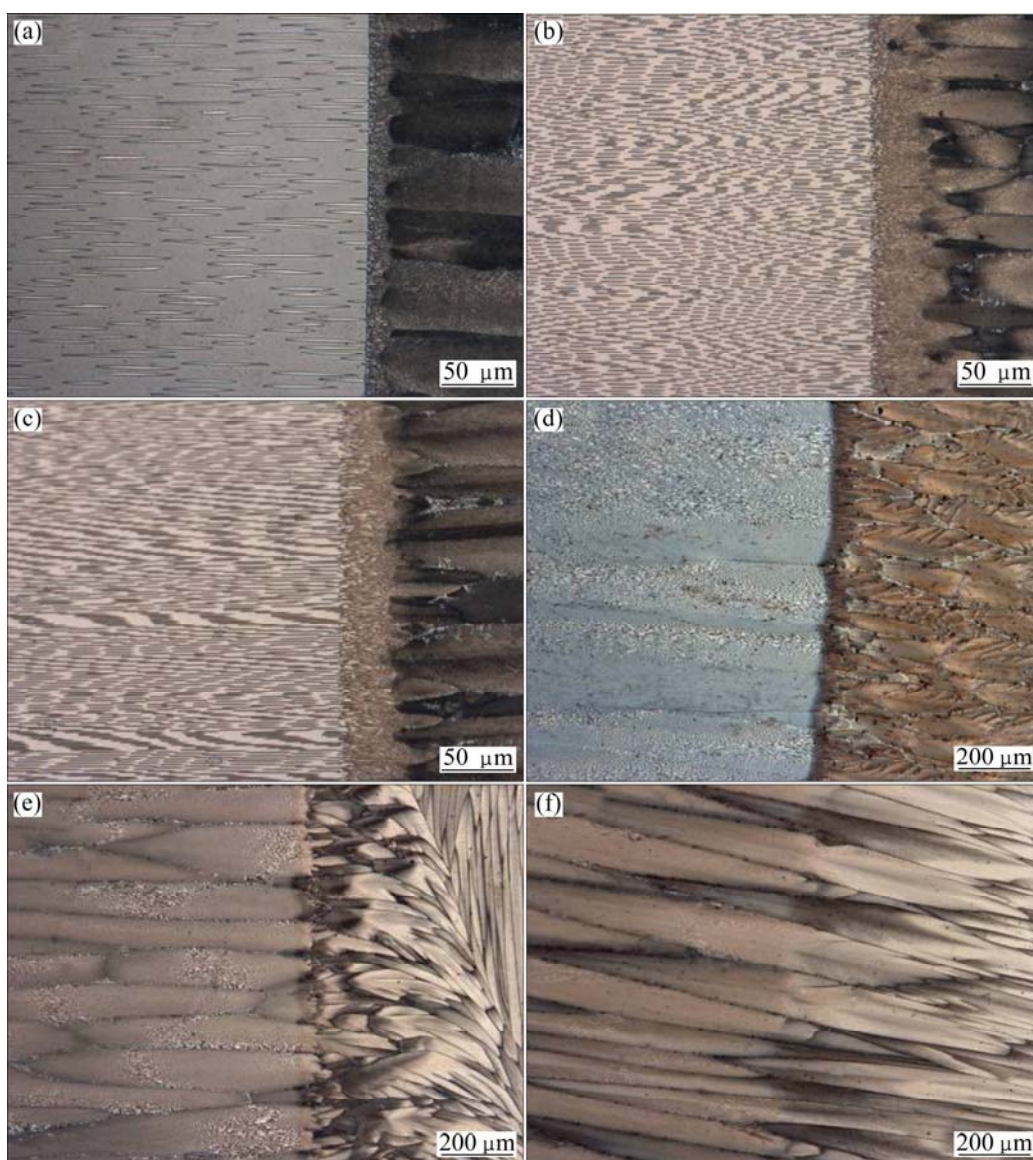


Fig. 1 OM images of solid/liquid interface under various growth rates: (a) $v=2 \mu\text{m/s}$; (b) $v=15 \mu\text{m/s}$; (c) $v=35 \mu\text{m/s}$; (d) $v=40 \mu\text{m/s}$; (e) $v=100 \mu\text{m/s}$; (f) $v=300 \mu\text{m/s}$ (Growth direction is from left to right)

the liquidus; D_L is the effective diffusion coefficient of solute atom in the liquid; C_E is the eutectic composition; C_0 is the initial composition of the solidifying alloy. Equation (1) shows that for a given growth rate, if there are no additional components, a large temperature gradient can keep planar interface and inhibiting colony formation. When Eq. (1) holds true, the interface is planar and the rod structure is obtained. When the growth rate is high enough to make Eq. (1) untenable, the interface evolves by the way from planar to cellular. It is observed that the evolution of steady-state S/L interface morphologies in this work is in concordance with the theory of crystal growth of the regular eutectic alloys [18]. Another point to note is that a third alloying element (such as impurities) which is similarly partitioned between both solid phases makes the S/L interface nonplanar, which leads to two-phase instability

and the appearance of eutectic cells or even eutectic dendrites [19].

3.2 Microstructure evolution of directionally solidified NiAl-9Mo alloy

Depending on the growth rates, two different steady-state growth morphologies were observed. For clarity, selected longitudinal and transverse microstructures of NiAl-9Mo alloy are shown in Fig. 2. The growth rates in a range from 2 to 35 $\mu\text{m/s}$ resulted in a very regular fibrous eutectic microstructure, as can be seen in Figs. 2(a)–(d). This is associated with a fact that the growth conditions are well controlled. In this case, the solidification process leads to cooperative growth of oriented structure, where both solid phases grow side by side. While the α phase segregates the constituent Ni and Al, the β phase rejects the constituent Mo. The

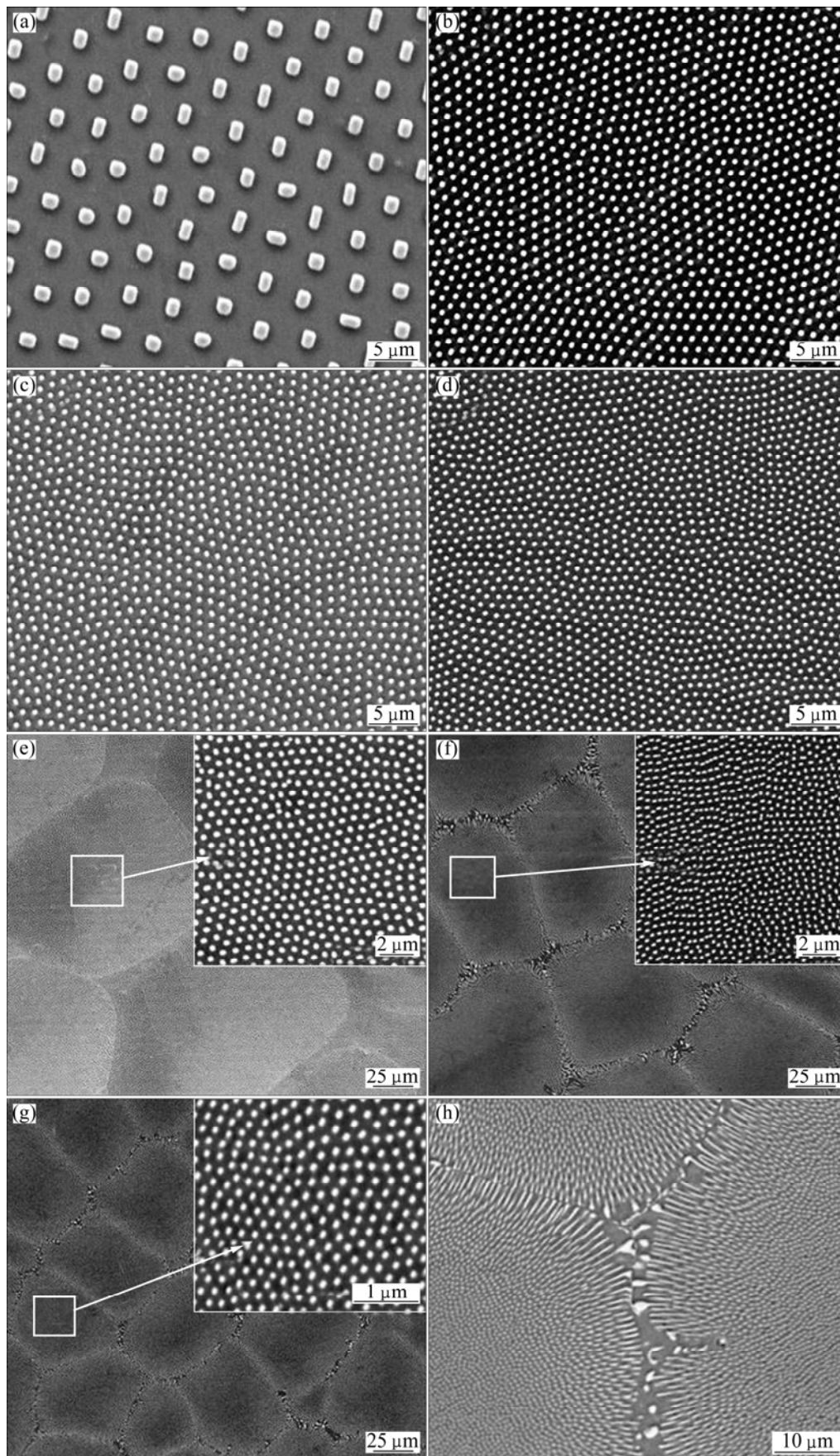


Fig. 2 Transverse microstructures of DS NiAl-9Mo alloy at different growth rates: (a) 2 $\mu\text{m/s}$; (b) 10 $\mu\text{m/s}$; (c) 25 $\mu\text{m/s}$; (d) 35 $\mu\text{m/s}$; (e) 40 $\mu\text{m/s}$; (f) 100 $\mu\text{m/s}$; (g) 300 $\mu\text{m/s}$; (h) Microstructure of cellular boundary

cooperative growth of the eutectic alloy is mainly a function of simultaneous diffusion ahead of the growth interface and efficient mass transport in the liquid ahead of the L/S interface. The arrangement of the Mo rods in the transverse section is approximately hexagonal. The shape of the rods is not circular in cross-section but rectangular. It suggests that the NiAl–Mo interfacial energy is highly anisotropic. The microstructures of the eutectic alloy solidified in the growth rates range from 40 to 300 $\mu\text{m/s}$ exhibited namely colony structures with fine fibrous morphology inside the colony and the coarse regions at colony boundaries (Figs. 2(e)–(g)). The characteristics of the colony structure have been observed that fibers do not grow parallel to each other within the cells, but diverge towards colony boundaries and tend to increase in thickness as they approach it (Fig. 2(h)).

The formation of a colony type structures depends on the growth mode, which depends on the solidification condition. It has been shown that the colonies are formed by the motion of a cellular S/L interface during growth. As mentioned before, there are two different reasons, which cause the instability of the planar eutectic interface. One dominant reason is the constitutional undercooling given by Eq. (1). A planar S/L interface becomes unstable when the growth rate is large enough that leads to the actual temperature gradient due to the heat flux, G_L , being lower than the liquidus temperature gradient at the S/L interface. In addition, the materials used in our work contain certain impurities (although the high purity materials are used and the quantities of impurities are very small), so the concentration of the impurities at the S/L interface also can provoke an additional constitutional undercooling. Under these conditions of growth, the planar S/L interface becomes unstable and transforms into cellular interface and consequently, leading to the formation of the cellular morphology and/or eutectic colonies.

The quantitative chemical composition analysis of regular fibers of Mo and NiAl matrix were carried out by EDS as shown in Fig. 3. Here the sample of $v=2 \mu\text{m/s}$ was selected to determine the compositions of the constituent phases. It was found that the NiAl matrix contained no Mo and had the off-stoichiometric composition Ni–45.09Al, whereas the Mo rods contained all three elements and had the composition Mo–14.69Al–12.55Ni.

3.3 Effect of growth rate on eutectic spacing

According to the spatial orientations of rods, the distance on a transverse section between the centers of adjacent Mo fibers was defined as the fiber spacing λ . And the average edge length of the square cross-sections d was used to characterize the scale of Mo rods. Now

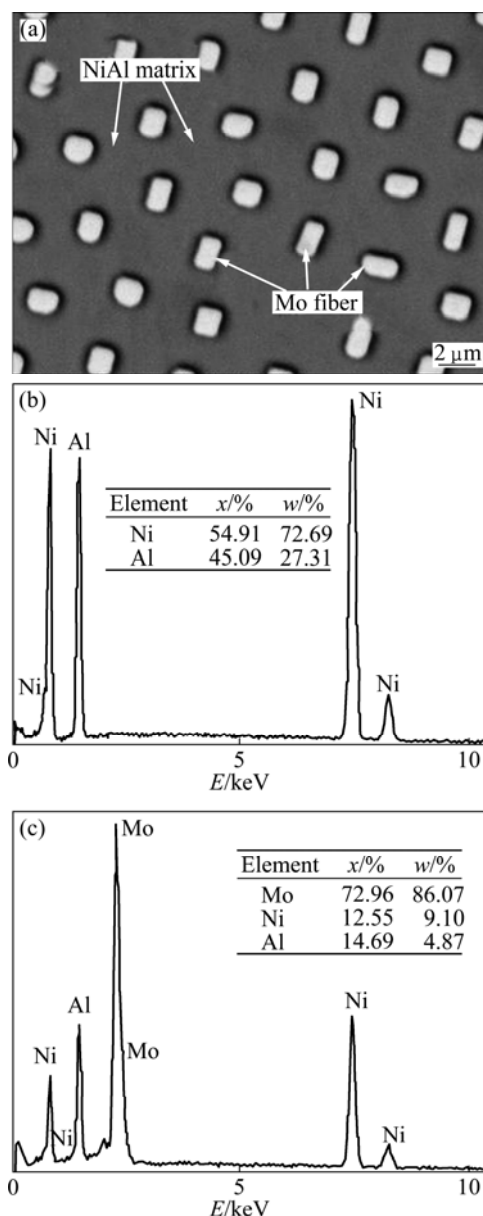
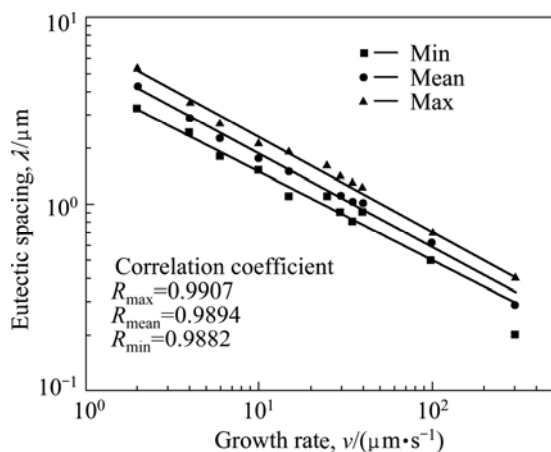


Fig. 3 SEM image (a) of NiAl–9Mo eutectic alloy and EDS analysis of matrix phase (b) and Mo fiber (c)

these two parameters will be used to quantitatively evaluate the effect of growth rate on the spacing and size of the rods. The eutectic spacing λ was determined by linear analysis of cross-section micrographs as listed in Table 1 and shown in Fig. 4. Owing to the radial nature of the fiber in the cellular boundary, the eutectic spacing λ was measured in the center of cells. As expected, the higher the growth rate is the finer the microstructure is. With increasing of growth rate, fiber spacing decreases. During eutectic growth of NiAl–Mo system, the solute atoms (Ni, Al and Mo), which are rejected by one phase, are usually needed for the growth of the other. Therefore, lateral diffusion along the S/L interface perpendicular to the fiber will become dominant and effectively decrease the solute build-up (ΔC) ahead of both phases. The fiber

Table 1 Experimental data of DS NiAl–9Mo alloy

Growth rate/ ($\mu\text{m}\cdot\text{s}^{-1}$)	Mo fiber spacing/ μm			Mo fiber size, $d/\mu\text{m}$	Interface morphology
	λ_{\min}	λ_{\max}	λ		
2	3.2	5.3	4.271	1.80	Planar
4	2.4	3.5	2.894	1.10	Planar
6	1.8	2.7	2.256	0.92	Planar
10	1.5	2.1	1.747	0.83	Planar
15	1.1	1.9	1.483	0.74	Planar
25	1.1	1.6	1.395	0.61	Planar
30	0.9	1.4	1.106	0.58	Planar
35	0.8	1.3	1.029	0.52	Planar
40	0.9	1.2	1.000	0.46	Cellular
100	0.5	0.7	0.615	0.28	Cellular
300	0.2	0.4	0.286	0.08	Cellular

**Fig. 4** Variation of eutectic spacing as function of growth rate at $G_L=334$ K/cm

spacing λ was decreased in the eutectic structure by the lateral diffusion.

It is found that the spacing at a given growth rate in the NiAl–9Mo system is not unique, but displays a limited range. The variation in the average eutectic spacing, maximum eutectic spacing and minimum eutectic spacing with the growth rates for the NiAl–Mo system is essentially linear on the logarithmic scale. The linear regression analysis gives the proportionality equation as follows:

$$\lambda = kv^{-n} \quad (\text{for constant } G) \quad (2)$$

where k is a constant and n is an exponent value of growth rate. As shown in Fig. 4, by linear regression analysis, the relationships between the eutectic spacings and growth rates were determined as follows:

$$\begin{aligned} \lambda_{\max} &= 7.29v^{-0.51}, \\ \lambda_{\text{mean}} &= 5.90v^{-0.50}, \\ \lambda_{\min} &= 4.45v^{-0.47} \end{aligned} \quad (3)$$

The value of exponent relating to the growth rates

(mean of 0.50) in the NiAl–Mo eutectic alloy obtained in this work is in good agreement with the value predicted by Jackson–Hunt (J–H) eutectic theory. Even the values of the exponent relating to the growth rates (maximum of 0.51) and (minimum of 0.47) are also very close to 0.50. The effect of the growth rate on rod spacing follows the classic relationship $v\lambda^2 = C$. The mean value of constant C was found to be $34.81 \mu\text{m}^3/\text{s}$. The constant obtained in this work is slightly larger than the constant of $26.50 \mu\text{m}^3/\text{s}$ and very close to the value of $33.94 \mu\text{m}^3/\text{s}$ obtained by BEI and GEDRGE [14] and ZHANG et al [20] for the same alloy system, respectively. These discrepancies in the values of $v\lambda^2 = C$ might be caused by the experimental conditions.

As we know, if the diffusion distance in the liquid is larger than the eutectic spacing, the system fulfils the J–H condition and the eutectic spacing λ depends on the growth rate v according to the J–H model [21]. Experiments on many system for eutectic spacing invariably confirm this relationship. It should be noted that the J–H model, $v\lambda^2 = C$, was originally developed for binary eutectic alloys with a planar eutectic microstructure. While in this work, the eutectic spacing λ was measured under not only planar microstructure but also non-planar microstructure. The NiAl–Mo system still fulfils the J–H condition and the eutectic spacing λ depends on the growth rate v . A similar relationship was also reported by RAJ and LOCCI [22] for NiAl–Cr(Mo) and RAJ et al [23] for NiAl–Cr(Mo) eutectic alloys with both planar and cellular eutectic microstructures. It is unclear that the form of J–H relationship is valid for these complex multicomponent eutectic alloys with cellular microstructure.

As listed in Table 1, with the increase of growth rate, Mo fiber size (d) is also decreased from $1.80 \mu\text{m}$ to $0.08 \mu\text{m}$. This also indicates that the rod scale is strongly dependent on the growth rate. Higher growth rates lead to a larger number of fibers that are finer and more dispersed over the NiAl matrix. Figure 5 shows a plot of the measured values of d as a function of growth rate v . As shown in Fig. 5, the data lie reasonably well on straight lines when d is plotted against the reciprocal of the square root of the growth rate $v^{-1/2}$. The relationship between v and d can be expressed as.

$$dv^{1/2} = 2.18 (\mu\text{m}^{3/2}\cdot\text{s}^{-1/2}) \quad (4)$$

3.4 Effect of growth rate on volume fraction of Mo phase

It can be seen that S/L interface remained planar at a macroscopic level only at velocities below $35 \mu\text{m}/\text{s}$. At velocities above this value the eutectic interface exhibited a tendency to assume a cellular morphology. In view of this transition from planar to cellular morphology

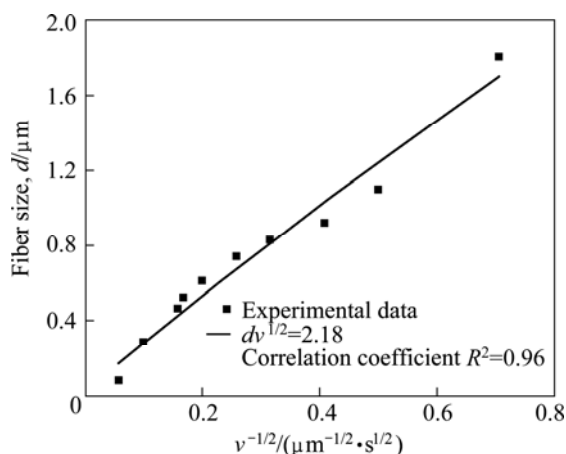


Fig. 5 Variation of fiber size as function of growth rate at $G_L=334$ K/cm

of the eutectic interface, all the Mo rod volume fraction data presented in this work were restricted to the velocity range of $2 \mu\text{m/s} \leq v \leq 35 \mu\text{m/s}$. Here, it is assumed that Mo fibers grow continuously at a constant diameter, then the volume fraction of Mo fibers is equal to their area fraction, which can be determined in turn from quantitative analysis of the SEM cross-sectional images. As shown in Fig. 6, application of SEM combined with image analysis measurements revealed that the volume fraction of the Mo phase slightly increased with the increasing of growth rate (from 2 to $35 \mu\text{m/s}$). The volume fraction of the Mo phase is not a constant but varied from 14.65% to 15.02% while the volume fraction of NiAl is reduced from 85.35% to 84.98%. This result reveals that at a constant G_L , the volume fraction of Mo phase can be varied in a certain extent in the NiAl–Mo eutectic system. Eutectic growth characterized by the co-operative growth of two solid phases from a liquid is an important issue in crystal growth. In the solidification process, both the nucleation rate and the growth rate of Mo phase are related with the undercooling and diffusion rate of solute in the liquid. As the growth rate increases, the undercooling in front of the S/L interface is increased. Increasing of the undercooling has the effect of increasing the nucleation rate and growth rate of Mo phase, whereas the diffusion rate of solute in the liquid is decreased, which can result in the increase of the density of Mo fibers. Another reasonable hypothesis for the variation of phase volume fraction for the NiAl–Mo eutectic microstructure perhaps involves the growth characteristics of the individual constituent phases. This eutectic is composed of Mo phase and intermetallic phase NiAl, while NiAl presents a high entropy of fusion [20]. According to RIOS et al [24], depending on the melting entropy of each phase, an increase in the growth rate restricts the growth of one phase, leading to an increase in the volume fraction of the other phase. This

phenomenon is also found in the Si–TaSi₂ eutectics [25] and NiAl–NiAlNb eutectics [26]. While in Fe–Cr–C eutectic composite [27], the volume fraction of carbide fibers was essentially the same, regardless of the growth rate. These results reveal that the fraction may be altered, depending on the growth rate and the nature of each phase. In addition, the solid solubilities of the eutectic phases in present work may be also a reason that contributes to the change of two-phase volume fraction.

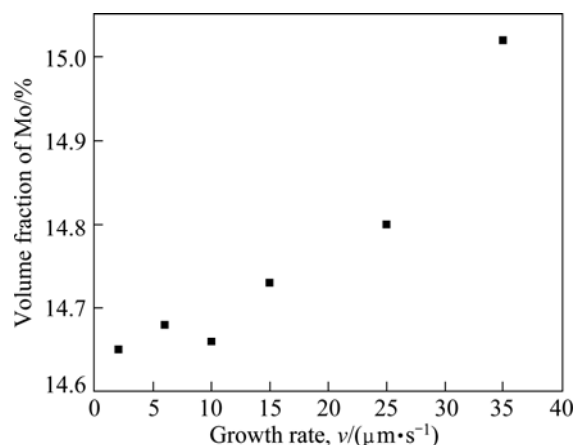


Fig. 6 Volume fraction of Mo phase as function of growth rate at $G_L=334$ K/cm

According to JACKSON and HUNT [21], when the volume fraction of the minor phase is smaller than 28%, the eutectic microstructure is of the fibrous type. In the case of eutectic alloy in the NiAl–Mo system, the largest volume fraction of the Mo phase is smaller than the mentioned value, and hence the eutectic microstructure formed by the NiAl phase and Mo phase is expected to present a fibrous morphology. In addition, the experimental results show that there is no fiber/lamellar transition with the increase in volume fraction of Mo phase in the present work.

4 Conclusions

1) Ni–45.5Al–9Mo alloy was directionally solidified under growth rates varying from 2 to $300 \mu\text{m/s}$. Regular and well-aligned rod-like eutectic structures were obtained under growth rates lower than $35 \mu\text{m/s}$.

2) With the increase of growth rate, two types of the solidified structures, planar and cellular, were identified for DS NiAl–9Mo alloy. The S/L interface evolution was in accordance with the classical eutectic growth theory.

3) The eutectic spacing was not a unique value but displayed a limited range for the rod-like NiAl–9Mo eutectic alloy for a given growth rate at a constant temperature gradient G_L . The relationships between eutectic spacing (λ), rod diameter (d) and growth rate (v) were obtained by binary regression analysis as:

$\lambda_{\max}=7.29v^{-0.51}$, $\lambda_{\text{mean}}=5.90v^{-0.50}$, $\lambda_{\min}=4.45v^{-0.47}$ and $dv^{1/2}=2.18(\mu\text{m}^{3/2}\cdot\text{s}^{-1/2})$. It is found that the mean value of the exponent relating to the growth rates of the NiAl–9Mo eutectic alloy is in good agreement with the value of 0.50 predicted by J–H eutectic theory with both planar eutectic and cellular microstructures.

4) The value of constant was also determined as $\lambda_{\text{mean}}^2 v = 38.41 \mu\text{m}^3/\text{s}$ by the measured values of λ_{Mo} . It was found that the value of constant obtained in this work was slightly larger than the value of $26.50 \mu\text{m}^3/\text{s}$ which is close to the value of $33.94 \mu\text{m}^3/\text{s}$ obtained by BEI and GEORGE and ZHANG et al for the same eutectic alloy, respectively.

5) The variation of the growth rates showed that an increase of this parameter implies an increase in the volume fraction of Mo phase, which is possibly attributed to an undercooling increases and the growth characteristics of the individual constituent phases during the eutectic growth.

References

- TANG L Z, ZHANG Z G, LI S S, GONG S K. Mechanical behaviors of NiAl–Cr(Mo)-based near eutectic alloy with Ti, Hf, Nb and W additions [J]. Transactions of Nonferrous Metals Society of China, 2010, 20(2): 212–216.
- XU G H, WANG G F, ZHANG K F. Effect of rare earth Y on oxidation behavior of NiAl–Al₂O₃ [J]. Transactions of Nonferrous Metals Society of China, 2011, 21(2): 362–368.
- WANG Z S, XIE Y, GUO J T, ZHOU L Z, HU Z Q, ZHANG G Y, CHEN Z G. High temperature oxidation behavior of directionally solidified NiAl–31Cr–2.9Mo–0.1Hf–0.05Ho eutectic alloy [J]. Transactions of Nonferrous Metals Society of China, 2012, 22(7): 1582–1587.
- MISRA A, GIBALA R, NOEBE R D. Optimization of toughness and strength in multiphase intermetallics [J]. Intermetallics, 2001, 9(10–11): 971–978.
- SHENG L Y, ZHANG W, GUO J T, YE H Q. Microstructure and mechanical properties of Hf and Ho doped NiAl–Cr(Mo) near eutectic alloy prepared by suction casting [J]. Mater Charact, 2009, 60(11): 1311–1316.
- ANVARI S Z, KARIMZADEH F, ENAYATI M H. Synthesis and characterization of NiAl–Al₂O₃ nanocomposite powder by mechanical alloying [J]. J Alloys Compd, 2009, 477(1–2): 178–181.
- SHENG L Y, ZHANG W, GUO J T. Microstructure and mechanical properties of NiAl–Cr(Mo)/Nb eutectic alloy prepared by injection-casting [J]. Mater Des, 2009, 30(4): 964–969.
- MILENKOVIC S, COELHO A A, CARAM R. Directional solidification processing of eutectic alloys in the Ni–Al–V system [J]. J Cryst Growth, 2000, 211(1–4): 485–490.
- VENKATESH T A, DUNAND D C. Reactive infiltration processing and secondary compressive creep of NiAl and NiAl–W composites [J]. Metall Mater Trans A, 2000, 31(3): 781–792.
- JOHNSON D R, CHEN X F, OLIVER B F, NOEBE R D, WHITTENBERGER J D. Processing and mechanical properties of in-situ composites from the NiAl–Cr and the NiAl–(Cr, Mo) eutectic systems [J]. Intermetallics, 1995, 3(2): 99–113.
- WHITTENBERGER J D, NOEBE R D, JOSLIN S M, OLIVER B F. Elevated temperature compressive slow strain rate properties of several directionally solidified NiAl–(Nb,Mo) alloys [J]. Intermetallics, 1999, 7(6): 627–633.
- ZHANG J F, SHEN J, SHANG Z, FENG Z R, WANG L S, FU H Z. Microstructure and room temperature fracture toughness of directionally solidified NiAl–Mo eutectic in situ composites [J]. Intermetallics, 2012, 21(1): 18–25.
- MISRA A, WU Z L, KUSH M T, GIBALA R. Microstructures and mechanical properties of directionally solidified NiAl–Mo and NiAl–Mo(Re) eutectic alloys [J]. Mater Sci Eng A, 1997, 239–240(4): 75–87.
- BEI H, GEORGE E P. Microstructures and mechanical properties of a directionally solidified NiAl–Mo eutectic alloy [J]. Acta Mater, 2005, 53(1): 69–77.
- FERRANDINI P, BATISTA W W, CARAM R. Influence of growth rate on the microstructure and mechanical behaviour of a NiAl–Mo eutectic alloy [J]. J Alloys Compd, 2004, 381(1–2): 91–98.
- EROL M, MARAŞLI N, KEŞLIOĞLU K, GÜNDÜZ M. Solid–liquid interfacial energy of bismuth in the Bi–Cd eutectic system [J]. Scripta Mater, 2004, 51(2): 131–136.
- FLEMINGS M C. Solidification processing [M]. New York: McGraw-Hill, Inc, 1974: 109.
- DAVIS S H, FREUND L B. Theory of solidification [M]. United Kingdom: Cambridge University Press, 2001: 267.
- KURZ W, FISHER D J. Fundamentals of solidification [M]. Switzerland: Trans Pub Ltd, 1998: 108.
- ZHANG J F, SHEN J, SHANG Z, FENG Z R, WANG L S, FU H Z. Regular rod-like eutectic spacing selection during directional solidified NiAl–9Mo eutectic in situ composite [J]. J Cryst Growth, 2011, 329(1): 77–81.
- JACKSON K A, HUNT J D. Lamellar and rod eutectic growth [J]. Trans Metall Soc AIME, 1966, 236: 1129–1141.
- RAJ S V, LOCCI I E. Microstructural characterization of a directionally-solidified Ni–33 (at.%) Al–31Cr–3Mo eutectic alloy as a function of withdrawal rate [J]. Intermetallics, 2001, 9(3): 217–227.
- RAJ S V, LOCCI I E, SALEM J A, PAWLIK R J. Effect of directionally solidified microstructures on the room-temperature fracture-toughness properties of Ni–33(at. pct)Al–33Cr–1Mo and Ni–33(at. pct)Al–31Cr–3Mo eutectic alloys grown at different solidification rates [J]. Metall Mater Trans A, 2002, 33(3): 597–612.
- RIOS C T, MILENKOVIC S, FERRANDINI P L, CARAM R. Directional solidification, microstructure and properties of the Al₃Nb–Nb₂Al eutectic [J]. J Cryst Growth, 2005, 275(1–2): 153–158.
- CUI C J, ZHANG J, JIA Z W, SU H J, LIU L, FU H Z. Microstructure and field emission properties of the Si–TaSi₂ eutectic in situ composites by electron beam floating zone melting technique [J]. J Cryst Growth, 2008, 310(1): 71–77.
- FERRANDINI P L, ARAUJO F L G U, BATISTA W W, CARAM R. Growth and characterization of the NiAl–NiAlNb eutectic structure [J]. J Cryst Growth, 2005, 275(1–2): 147–152.
- LU L M, SODA H, MCLEAN A. Microstructure and mechanical properties of Fe–Cr–C eutectic composites [J]. Mater Sci Eng A, 2003, 347(1–2): 218.

定向凝固 NiAl-9Mo 共晶合金的凝固组织特性

张建飞^{1,2}, 沈军¹, 商昭¹, 王雷¹, 傅恒志¹

1. 西北工业大学 凝固技术国家重点实验室, 西安 710072;

2. 内蒙古科技大学 材料与冶金学院, 包头 014010

摘要: 采用液态金属冷却法在恒定温度梯度 $G_L=334$ K/cm, 大生长速率范围内(2~300 $\mu\text{m/s}$)对 Ni-45.5Al-9Mo (摩尔分数, %)共晶合金进行定向凝固制备。研究生长速率(v)对纤维间距(λ)、纤维直径(d)和纤维体积分数的影响。在实验中发现平界面和胞界面两类共晶生长界面。在平界面和胞界面组织中, 生长速率(v)与纤维间距(λ)和纤维直径(d)的关系经回归分析分别为: $\lambda v^{1/2}=5.90 \mu\text{m}\cdot\mu\text{m}^{1/2}\cdot\text{s}^{1/2}$ 和 $d v^{1/2}=2.18 \mu\text{m}\cdot\mu\text{m}^{1/2}\cdot\text{s}^{1/2}$ 。Mo 纤维的体积分数可在一定的范围内随生长速率进行调整, 这是由生长过程中界面前沿过冷度的增加及共晶组织中各组成相的生长特性引起的。

关键词: NiAl-9Mo; 定向凝固; 金属间化合物; 晶体生长; 微观组织

(Edited by Chao WANG)